Video Article

Implementation of a Coherent Anti-Stokes Raman Scattering (CARS) System on a Ti:Sapphire and OPO Laser Based Standard Laser Scanning Microscope

Vasyl Mytskaniuk*[1], Fabrice Bardin*[2,3], Hassan Boukhaddaoui[1,5], Herve Rigneault[4], Nicolas Tricaud[1]

[1]INSERM U1051, Institut des Neurosciences de Montpellier (INM), Université de Montpellier

[2]Université de Nîmes

[3]CNRS, IES, UMR 5214

[4]Aix-Marseille Université, CNRS, École Centrale Marseille, Institut Fresnel, UMR 7249

[5]Montpellier RIO Imaging (MRI)

*These authors contributed equally

Correspondence to: Fabrice Bardin at fabrice.bardin@unimes.fr

URL: https://www.jove.com/video/54262
DOI: doi:10.3791/54262

Keywords: Biophysics, Issue 113, Cellular biology, Coherent anti-Stokes Raman scattering, microscopy, laser scanning microscope, nonlinear imaging, in-vivo imaging, lipid, myelin

Date Published: 7/17/2016

Citation: Mytskaniuk, V., Bardin, F., Boukhaddaoui, H., Rigneault, H., Tricaud, N. Implementation of a Coherent Anti-Stokes Raman Scattering (CARS) System on a Ti:Sapphire and OPO Laser Based Standard Laser Scanning Microscope. *J. Vis. Exp.* (113), e54262, doi:10.3791/54262 (2016).

Abstract

Laser scanning microscopes combining a femtosecond Ti:sapphire laser and an optical parametric oscillator (OPO) to duplicate the laser line have become available for biologists. These systems are primarily designed for multi-channel two-photon fluorescence microscopy. However, without any modification, complementary non-linear optical microscopy such as second-harmonic generation (SHG) or third harmonic generation (THG) can also be performed with this set-up, allowing label-free imaging of structured molecules or aqueous medium-lipid interfaces. These techniques are well suited for *in-vivo* observation, but are limited in chemical specificity. Chemically selective imaging can be obtained from inherent vibration signals based on Raman scattering. Confocal Raman microscopy provides 3D spatial resolution, but it requires high average power and long acquisition time. To overcome these difficulties, recent advances in laser technology have permitted the development of nonlinear optical vibrational microscopy, in particular coherent anti-Stokes Raman scattering (CARS). CARS microscopy has therefore emerged as a powerful tool for biological and live cell imaging, by chemically mapping lipids (via C-H stretch vibration), water (via O-H stretch vibrations), proteins or DNA. In this work, we describe the implementation of the CARS technique on a standard OPO-coupled multiphoton laser scanning microscope. It is based on the in-time synchronization of the two laser lines by adjusting the length of one of the laser beam path. We present a step-by-step implementation of this technique on an existing multiphoton system. A basic background in experimental optics is helpful and the presented system does not require expensive supplementary equipment. We also illustrate CARS imaging obtained on myelin sheaths of sciatic nerve of rodent, and we show that this imaging can be performed simultaneously with other nonlinear optical imaging, such as standard two-photon fluorescence technique and second-harmonic generation.

Video Link

The video component of this article can be found at https://www.jove.com/video/54262/

Introduction

Optical microscopy has become a major technique for nondestructive visualization of dynamic processes in living biological systems with a subcellular resolution. Fluorescence microscopy is currently the most popular imaging contrast used in live cells due to its high specificity and sensitivity[1]. A large palette of fluorescent probes has emerged (exogenous dyes, genetically encoded proteins, semiconductor nanoparticles). Various sample illumination fluorescent-based techniques have flourished (such as confocal or two-photon microscopy) to perform 3D imaging and to reduce a main drawback of this technique which is photobleaching[2]. Other limitations include the requirement of fluorophore labeling because most of molecular species are not intrinsically fluorescent and therefore these fluorophores have to be artificially introduced in the imaged sample. This artificial manipulation may be disruptive especially for small molecules or induces potential photo-toxicity. These reasons make fluorescence microscopy not well suited for *in-vivo* observations. Hence, the use of optical imaging techniques with high sensitivity and specific molecular contrasts without the use of fluorescent molecules is highly desirable in biomedical science.

Several nonlinear optical imaging techniques without labeling or staining have emerged, including second-harmonic generation (SHG)[3,4] and third-harmonic generation (THG)[5]. SHG microscopy has been used to image structural arrangements at the supramolecular level such as microtubules or collagen[6]. THG is generated from optical heterogeneities such as interface between an aqueous medium and lipids[7]. THG was also demonstrated to image myelin[8,9]. Both techniques can be implemented on a two-photon fluorescence microscope and require only one

laser beam. However they require high power laser intensity (typically 50 mW at 860 nm for SHG[10], 25 - 50 mW at 1,180 nm for THG[9]), which is deleterious in living samples, and do not provide the chemical specificity that is required to unambiguously image specific biological structures.

Chemically selective imaging can be obtained from inherent molecular vibration signals based on Raman scattering. When a beam of light hits matter, photons can be absorbed and scattered by atoms or molecules. Most of the scattered photons will have the same energy, *i.e.,* frequency, as the incident photons. This process is called Rayleigh scattering. However, a small number of photons will be scattered at an optical frequency different from the frequency of the incident photons, *i.e.,* with an inelastic scattering process called Raman scattering. The difference in energy originates from excitation of vibrational modes depending on molecular structure and environment. Therefore, spontaneous Raman scattering provides chemically selective imaging as different molecules have specific vibrational frequencies. However it is limited because of its extremely weak signal. Confocal Raman microscopy has been developed and provides 3D spatial resolution, but it requires high average power and long acquisition time[11]. To overcome these difficulties, recent advances in laser technology have allowed the rise of nonlinear optical vibrational microscopy, in particular coherent anti-Stokes Raman scattering (CARS)[11,12,13].

CARS is a third-order nonlinear optical process. Three laser beams, composed of a pump beam at frequency ω_P, a Stokes beam at frequency ω_S and a probe beam (most often being the pump) are focused in a sample and generate an anti-Stokes beam at frequency $\omega_{AS}= (2\omega_P - \omega_S)$[14]. The anti-Stokes signal can be significantly enhanced when the frequency difference between the pump and the Stokes beams is tuned to a Raman molecular vibration $\Omega_R=(\omega_P - \omega_S)$. CARS signal is based on multiple photon interaction. It generates therefore a coherent signal orders of magnitude stronger than spontaneous Raman scattering.

CARS microscopy was first experimentally demonstrated by Duncan *et al.*[15]. Zumbusch *et al.* improved then the technique, by using two focused near-infrared femtosecond laser beams with an objective lens of high numerical aperture, allowing the phase matching condition of CARS and avoiding the two-photon non-resonant background[16]. CARS microscopy has therefore emerged as a powerful tool for live cell and tissues imaging, by chemically detecting molecules such as lipids (via C-H stretch vibration)[17,18], water (via O-H stretch vibrations), proteins, DNA in live cells[19,20] but also deuterated chemical compounds for pharmaceutical[21] and cosmetic applications[22].

The major limitation of nonlinear microscopy originates from the complexity and the cost of the optical sources. A CARS system requires two wavelength tunable lasers with short pulse durations and with temporally and spatially synchronized pulse trains. Early CARS microscopes were based on two synchronized picosecond Ti:sapphire lasers[20]. CARS imaging was also obtained from a single femtosecond Ti:sapphire laser generating a supercontinuum light source[23]. Recently, laser sources composed of a single femtosecond Ti:sapphire laser pumping a tunable optical parametric oscillators (OPO) have been used for CARS microscopy. This set-up allows intrinsically temporally synchronized beams with a difference of frequency between the pump and the Stokes beam covering the full molecular vibrational spectrum[24]. In addition, laser scanning microscopes based on a turn-key fs laser and an OPO, primarily used for two-photon fluorescence (TPF) are now available for non-physicists. The potential of such set-ups can be greatly enhanced without requiring supplementary investment by the incorporation of other nonlinear optical imaging, since each nonlinear (NLO) imaging modality is sensitive to specific structures or molecules. Multimodal NLO imaging therefore capitalizes the potential of NLO microscopy for complex biological samples[25]. The coupling of these techniques has allowed the investigation of many biological questions, in particular on lipid metabolism, skin or cancer development[26], skeletal muscle development[27], atherosclerotic lesions[28]. Moreover, the implementation of laser beam scanning with CARS gives the capability of high-rate imaging, *i.e.,* an appealing tool to study dynamical processes *in vivo*.

The aim of this work is to show each step to implement the CARS technique on a standard multiphoton laser scanning microscope. The microscope is based on a fsec Ti:sapphire laser and an OPO (pumped by the Ti:sapphire laser) operated by a software for biologists. The integration was performed by adjusting the length of one of the laser beam path in order to synchronize in time the two beams. We describe the step-by-step implementation of this technique which requires only basic background in experimental optics. We also illustrate CARS imaging obtained on myelin sheaths of sciatic nerve of rodents, and we show this imaging can be performed simultaneously with other nonlinear optical imaging, such as standard two-photon fluorescence technique and second-harmonic generation.

Protocol

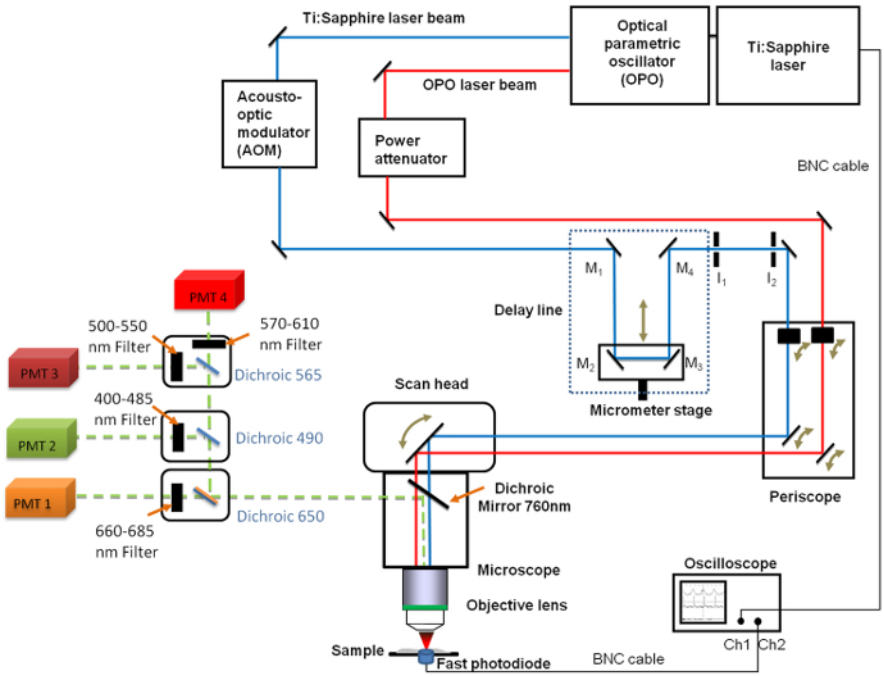

Figure 1. Schematic view of the general set-up. It includes the Ti:sapphire (680 - 1,080 nm) and the OPO (1,050 - 1,300 nm) lasers, the delay line with the 4 mirrors (M_1 to M_4), the fast oscilloscope, the photodiode and two fixed iris diaphragms I_1 and I_2. Mirrors M_2 and M_3 are fixed on a linear translation stage enabling to change the delay line length with a micrometer resolution. A 660 - 685 nm band pass filter was positioned in front of the PhotoMultiplier Tube (PMT) used for CARS imaging. Please click here to view a larger version of this figure.

1. Startup of the Laser System

1. Verify that the Ti:sapphire wavelength is set to 800 nm or define this wavelength on the Ti:sapphire power supply controller. Turn the key from Standby to On to switch on the Ti:sapphire laser.
2. Turn on the OPO laser at the back of the OPO controller and open the Ti:sapphire shutter on the Ti:sapphire power supply controller.
3. Switch on the tablet computer to pump up the OPO. Click on the OPO Connected and Remote Connected icons on the tablet. Wait for 30 - 40 min for warming up.
4. Switch on the microscope computer and turn on the "Microscope Components" switches. Start the software by double clicking the icon on the desktop.
5. Into the software Acquisition tab, open the **Laser tool** in the **Setup Manager** to operate both lasers from the software. Select Ti:sapphire laser **On** and OPO laser **On**. Check the value of the optical laser power (typical values of 3,700 mW at 800 nm and 700 mW at 1,000 nm).
6. To configure the beam path and lasers, open the **Light Path tool** in the **Setup Manager tool** group and check box **the first Photomultiplier tube** (PMT).
7. To check the Ti:sapphire laser spot at the output of the objective, open the **Channels tool** in the **Acquisition Parameter tool** group. Select the Ti:sapphire power at low value (around **1%**), reduce the gain to 0 (no image is needed at this stage) and click on the **Continuous** button to start the scanning procedure to launch the laser beam through the microscope objective. Check the presence of a red spot by direct observation by positioning the IR laser viewing card at the output of the air microscope objective (10X).
8. To check the OPO laser spot, stop the scan of the Ti:sapphire laser by clicking on the **Stop** button. Select the **OPO power** at low value in the **Channels window** and click on the **Continuous** button.

2. Microscope Settings

1. Manually place the dichroic mirror with a cutoff wavelength at 760 nm in the sideport slider in the infinity space above the objective nosepiece to launch the light up to 760 nm from the sample into the PMTs in non-descanned detection (NDD) mode.
2. Set the narrow band pass filter at 660 - 685 nm in the NDD reflector cube in front of PMT1 to record only the CARS signal at 670 nm to reproduce the results presented in this work.
3. Place a narrow band filter ranging from 500 to 550 nm in the NDD reflector cube in front of PMT3 for fluorescence observation of the myelin. Place a narrow band filter ranging from 565 to 610 nm in the reflector cube in front of PMT4 for SHG observation.
4. To select in the software the recording of the signal on the detector with the *ad hoc* band pass filter, open the **Light Path tool** in the **Setup Manager menu** in the **Acquisition tab**. Activate the desired PMT (check box) and select a color for this channel. In this work, the green was chosen for CARS, red for fluorescence and magenta for SHG.

3. Temporal Synchronization

Note: The two laser beams originate from the same Ti:sapphire laser but the OPO beam is delayed when it is generated so the two beams are not synchronized in time when they reach the microscope. The goal here is to delay one of the two beams to re-synchronize them in time before they reach the microscope.

1. Connect with BNC cables the input channel CH1 of the oscilloscope to the electrical BNC laser output (Sync. Out). Connect the input channel CH2 of the oscilloscope to the photodiode and choose the CH1 channel as the trigger channel by pressing **TRIGGER MENU**, then the main-menu button Source and then the side-menu button that corresponds to the channel selected CH1.
2. Position and fix with optical mounting posts the photodiode in the focal plane of an air microscope objective (10X) or in the beam path of the microscope after removing the objective. Note: If necessary, remove the condenser and its carrier.
3. In the **Channels** tool (**Acquisition Parameter tool** group), define the Ti:sapphire laser wavelength at 830 nm at low power (*i.e.,* less than **1%** of the full power). In the **Acquisition Mode tool**, reduce the scan area to one point in order to illuminate the photodiode with the tiniest beam. Switch on the laser scan by clicking on the **Continuous button**.
4. Press **AUTOSET** on the oscilloscope front panel and manually move the position of the photodiode to get the pulse trains on the screen. Press **RUN/STOP** button to freeze the display.
    1. To save a copy of the oscilloscope display, insert a 3.5 inch floppy disk in the floppy disk drive or connect the GPIB port on the rear panel to a computer. Then press **SHIFT HARDCOPY MENU**, press **FORMAT** (main) to select **TIFF** image format and specify in the Port menu the output channel. Press **HARDCOPY** button to record the oscilloscope display of the pulse trains of the Ti:sapphire laser.
5. Switch off the Ti:sapphire laser scan by clicking on the **Stop** button. By clicking **Channels tool** define the OPO signal at 1,107 nm and low power. Switch on the OPO laser scan and record the pulse trains of the OPO laser on the oscilloscope. Switch off the OPO laser scan.
6. Compare the temporal shift between the Ti:sapphire and the OPO signals.
   NOTE: The temporal shift t_{shift} gives the length of the delay line $L_{DelayLine}$ which has to be implemented following the equation: $L_{delayLine} = c \times t_{shift}$ where c is the speed of light.
7. Choose one of the laser lines.
   NOTE: In this work, the Ti:sapphire laser line was chosen because free space was available near this laser line. In addition, this choice allows to achieve the re-alignment of the laser line with a visible laser light.
8. Open the laser line by removing the protective tubes at the position where the delay line will be implemented.
   Caution! Wear appropriate safety goggles and remove chain bracelets or watch from wrists.
9. Select a wavelength in the visible range in order to be able to easily observe the laser beam (700 nm for instance, at low power in the **Channels tool** of the software). Switch on the laser scan.
10. Place and set with optical mounting posts two iris diaphragms along the open laser line. Position one iris at the exit of the delay line and place the other iris at the entrance of the periscope.
    NOTE: The periscope controls by two motorized mirrors piloted by the software the angle of entrance of the laser beam into the scanning head of the laser scanning microscope.
11. Decrease the iris diaphragm aperture and adjust the diaphragm positions to fit the laser beam path. Fix them on the optical table. Adjust the vertical position of a third mobile iris diaphragm, to check the height of the laser beam while successively positioning the four mirrors of the delay line.
    NOTE: These iris diaphragms will serve as control for the re-alignment procedure by showing the path to follow.
12. Place the mirror M1 mounted on a compact kinematic mirror mount at the entrance of the delay line (as shown in **Figure 1**) and adjust its position and its orientation to maintain the beam height with the use of the mobile iris diaphragm. Place mirrors M2 and M3 (also mounted on compact kinematic mirror mounts) at 90° onto the translation stage which will be positioned at midcourse. Position them to fit the delay line length as previously calculated.
13. Adjust the orientation of M2 and M3 with the use of the mobile iris diaphragm. Set M4 (also fixed on a compact mount) at the exit of the delay line (just before iris I_1 as shown in **Figure 1**) and carefully adjust its position and angle to fit the laser beam path through the two fixed iris diaphragms.
14. Position the laser viewing card at the output of the microscope objective and check the laser beam profile by clicking on **Continuous** to turn on the laser scan. Observe a uniform bright disk. If necessary, slightly adjust the orientation of M4.
15. Position again the fast photodiode under the laser beam in the sample focus plane of the microscope. Observe the temporal shift between the Ti:sapphire laser beam and the OPO beam on the oscilloscope.
    Note: If necessary, change the delay line length by moving the whole system M2, M3 mounted on the translation stage (without changing the translation stage tuning) to synchronize both pulses. Changes of few centimeters can be required.

4. Spatial Overlap of the Beams

Note: To produce a CARS signal, the spatial overlapping of the two laser beams is required. The alternate illumination of both beams on the same beads stained throughout with two different fluorescent dyes can be used to indicate the spatial shift. Fine adjustments of the mirror positions can then minimize the shift.

1. Use pre-mounted fluorescent microspheres. Or mount microspheres in suspension on clean microscope slides as described below:
    1. Before sampling, mix (on a cortex mixer or by sonicating) the beads solution to be sure that the beads are uniformly suspended.
    2. Apply 5 µl of the bead suspension to the surface of a slide and spread with the pipette tip. Wait for the droplet to dry and then apply 5 µl of mounting medium, such as glycerol, water or immersion oil over the dry sample of beads. Cover the sample with a coverslip and seal the coverslip with quick-drying glue or melted paraffin.
2. Place the fluorescent polystyrene beads fixed on a microscope slide under the 20X water objective. Add few drops of water to immerse the objective.

3. To achieve the focus on the beads, open the **Locate** tab in the software to switch from the laser scanning mode to the direct observation of the sample with the eye, by pressing the **Online** button. Open the **Ocular tool** to select the ***ad hoc* filter** and switch on the halogen lamp by clicking on **icons**.
4. Manually remove the dichroic mirror in the sideport slider in infinity space and use the focusing drive of the microscope to focus the sample plane by observing the beads with the oculars. Replace the dichroic mirror.
5. In the **Locate tab**, switch to the laser scanning mode by pressing the **Offline** button. Go to the **Acquisition tab** to define the parameters for scanning: select the frame size to 512 pixels, a scan speed of 9, an averaging of 1, a bit depth of 8 bit and increase the scan area to the maximum.
6. In the **Channels tool** of the **Acquisition tab**, add a Track (Track 1) if not already created. Select the wavelength at 830 nm and low power for the Ti:sapphire laser beam. **Tick** the color to green in the Track 1 box from the Channels window and in the PMT3 or the PMT4 box from the Light Path window.
7. In the **Channels tool** of the **Acquisition tab**, add a second Track (Track 2). Select the wavelength at 1,107 nm and low power for the OPO laser beam. Tick the color to red in the Track 2 box from the **Channels window** and in the PMT3 box from the **Light Path window**.
8. Adjust the gain of both tracks to 600. Then, sequentially apply the scan of the two beams onto the sample by clicking on **Continuous**.
9. Observe the image in the screen area into the 2D view. In the **Display View Option** control block, adjust the display intensity.
   Note: If necessary, move slightly the focusing drive to find the focus plane of the beads. Adjust the Crop and zoom the image in a single bead or in a group of adjacent beads.
10. Use the periscope controller to overlap the beams in x-y plane. In the software, open the **Maintain tab**. Click on the **System Options** and display the **Motorized Periscope tool** window. Use coarse and fine adjustments of the periscope mirrors of the Ti:sapphire laser beam in order to synchronize in space both images.
11. For the periscope manipulation, use the first adjustment bars for vertical and the second one for horizontal movements of the laser beam. Move the beam with the input mirror until the image is slightly visible, and then compensate for the laser intensity with the output mirror of the periscope by clicking on "input" and "output".
12. In order to vertically overlap the beams, in the **Maintain tab**, open the **Collimator tool** and adjust the value of the focal distance of the Ti:sapphire laser beam.
13. Move gently the objective vertical position to check the difference of focus on both images. Or, take a z-stack of the sample by opening in the Acquisition tab the Z-Stack tool and choose the different parameters (range, number of slices). Press Ortho in the image screen area to see the beams in axial cross-section. Maximize the z-overlap by doing the same procedure several times.

5. Final Adjustments and Coherent Anti-Stokes Raman Scattering (CARS) Signal Observation from Olive Oil Droplets

1. Put a droplet of olive oil on a glass plate and cover it by a glass cover slip. Add few drops of water to immerse a 20X water immersion objective. Focus at the edge of the cover slip by using the oculars (as explained previously in 4.2).
2. In the **Channels tool** of the **Acquisition tab**, select in Track 1 the wavelength at 830 nm for the Ti:sapphire laser beam and at 1,107 nm for the OPO. Tick both lasers in Track 1 to get a simultaneous scan of both lasers. Set powers at low value for a start.
3. In the **Light Path window**, select PMT1. Switch on the laser scans by clicking on the **Continuous** button. Move slightly the focus to deliver the laser light into the oil thin layer.
4. If necessary, increase the optical power of both lasers. Adjust the display intensity in the Display View Option control block. Slowly move the translation stage of the delay line until the signal becomes significantly enhanced.
5. After the fine alignments are complete, check whether it is really a CARS signal: Move slightly the translation stage; the intensity of the signal must become weaker. And/or switch off one of the laser beam, either Ti:sapphire laser or OPO. Again there must be a strong decay in intensity compared to the CARS signal.
6. To achieve the maximum CARS signal, select the option on the software to provide a value of the mean intensity of the whole image (in the Histo view of the screen area tab). Adjust the wavelength (few nm), then the x,y,z positions of the focus beam to maximize the mean intensity value.

6. Enclosure of the Light Path of the Delay Line

1. Since the final system is dedicated to non-physicists, enclose the light path of the delay line with tubes or an enclosure box, to avoid direct access to harmful non-visible high peak power laser beam. Take care to provide an access to the translation stage knob.

7. Wavelength Tuning for CARS

1. Use the equation $\Omega_R = \frac{1}{\lambda_P} - \frac{1}{\lambda_S} = \frac{1}{\lambda_{Ti:sapphire}} - \frac{1}{\lambda_{OPO}}$ to tune the laser wavelengths to the desired Raman vibration. To reproduce the results presented in this work to image CARS signal from C-H bonds having stretching vibration of 3015 cm^{-1}, select $\lambda_{Ti:sapphire}$ = 830 nm and λ_{OPO} = 1,095 nm.
   NOTE: Raman characteristic vibrational frequencies observed in biological samples, such as water, C-H bond can be found in Evans *et al.*[13] or in Ellis *et al.*[29].
2. Use the equation $\lambda_{CARS} = 1/\left(\frac{2}{\lambda_P} - \frac{1}{\lambda_S}\right) = 1/\left(\frac{2}{\lambda_{Ti:sapphire}} - \frac{1}{\lambda_{OPO}}\right)$ to determine the emission wavelength of CARS signal. For C-H bond imaging by CARS, choose a narrow band filter at 670 nm since λ_{CARS} = 670 nm with laser wavelengths presented in 7.1.
   NOTE: A mobile phone application is available to calculate λ_{CARS} from λ_P and λ_S values (see reference 30).

8. Observation of CARS Signal and Stained Myelin from Sciatic Nerve Cuts

Note: All animal experiments were conducted in accordance with institutional regulations.

1. Prepare the axial and longitudinal sciatic nerve cuts on a microscope slide as presented in Ozçelik *et al.*[31].
2. Prepare the fluoromyelin red staining solution by diluting the stock solution 300-fold into PBS. Flood the nerve cuts with the staining solution for 20 min at RT. Remove the solution and wash 3 times for 10 min with PBS.
3. Position the cuts under the 20X water immersion objective. Place a coverslip. Add few drops of PBS to immerse the objective and adjust the focus of the objective to obtain a clear image of the cuts through the oculars (as previously detailed in 4.2).
4. In Track 1, select the Ti:sapphire and the OPO lasers and define their wavelengths to **830 nm** and **1,095 nm**, respectively. In the **Light Path window**, select **PMT1** and green color.
5. In Track 2, select the OPO laser only (wavelength at **1,095 nm**). In the **Light Path window**, select **PMT4** and red color.
6. For both lasers, select low power and set the gain to 600 for a start. Switch on the laser scans and adjust the following parameters to improve CARS and fluorescence signal contrasts: power values, translation stage knob (very slightly), wavelengths (few nm), display intensity.
7. To record final images at high resolution, select in the **Acquisition Mode tool** the following parameters: frame size of 1,024 pixels, scan speed of 7, averaging of 4. Click on the Snap button for recording a single image. Save the image in the proprietary format to record the image and the full acquisition parameters.

9. Observation of CARS and SHG Signals from Sciatic Nerve Cuts

1. Prepare the sciatic nerve as presented in Ozçelik *et al.*[31].
2. Follow the procedure as explained in part 8 to get an image through the oculars and to select CARS signal parameter (Track 1).
3. In Track 2, select the OPO laser only (wavelength at **1095 nm**). In the **Light Path window**, select PMT3 and magenta color.
4. Follow the procedure as explained in part 8 to switch on the laser scans and save high resolution images.

Representative Results

The pulse train frequency of standard Ti:sapphire laser is typically around 80 MHz. The OPO has the same frequency since it is pumped by the Ti:sapphire laser. A fast oscilloscope of at least 200 MHz is therefore required. A fast photodiode in the range 600 to 1,100 nm is also required. The maximal temporal shift occurs when the Ti:sapphire and the OPO signals are shifted of $1/(2\times80\times10^6) = 6.2$ nanoseconds. It corresponds to a maximum beam path shift of 1.9 m. **Figure 2** shows the pulse train recorded from the OPO laser beam (A) and from the Ti:sapphire laser beam without the delay line (B) and with the adjusted delay line (C). The pulse trains are thus roughly synchronized in time with the implemented delay line as shown in **Figure 2A** and **2C**.

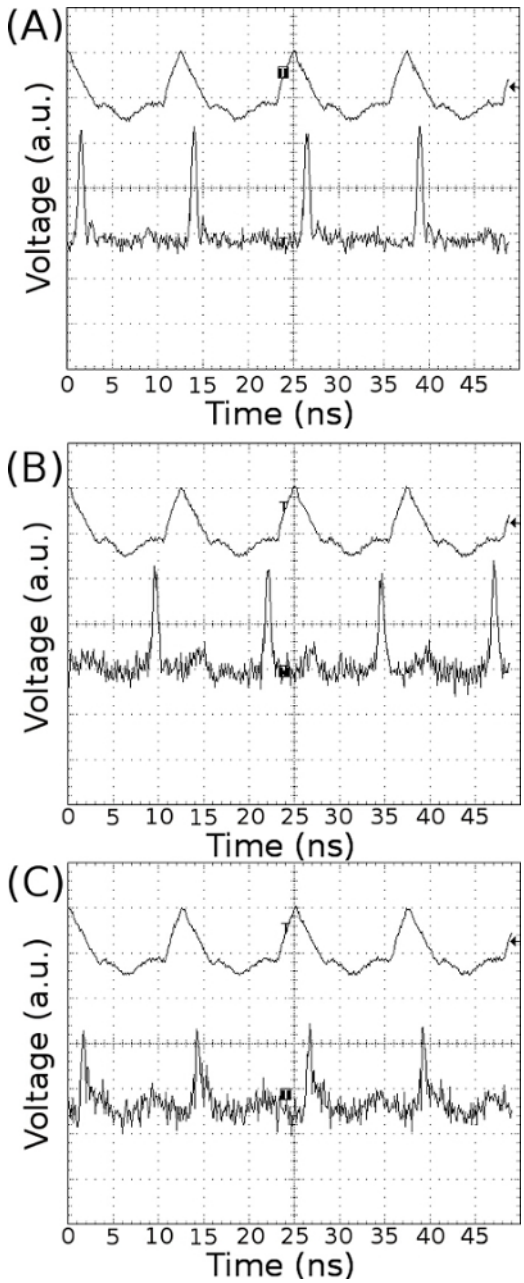

Figure 2. Laser pulse train recordings for the temporal synchronization. Recording of pulse trains at the microscope sample plane with a 10X objective of the OPO beam (**A**), the Ti:sapphire laser beam without (**B**) and with the delay line (**C**). The top curve of each graph plots the signal directly recorded from the BNC connector on the back of the Ti:sapphire laser (Sync. out connector). The oscilloscope trigger is adjusted on this signal. Please click here to view a larger version of this figure.

The spatial overlap of the two beams can be obtained by the visualization of fluorescent polystyrene beads fixed on top of a microscope slide (**Figure 3A**). **Figure 3B** shows the image of three nearby beads given by the OPO laser at 1,107 nm (red false color) and by the Ti:sapphire laser at 830 nm (green false color). The spatial shift between both laser beams has been compensated following the procedure of the spatial synchronization previously described (**Figure 3C**).

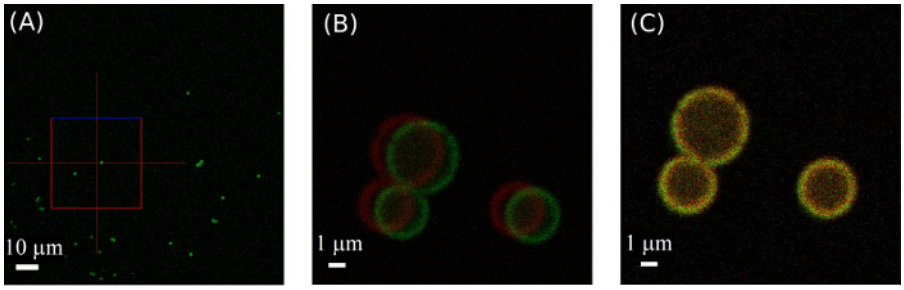

Figure 3. Spatial overlap of the beams. General view of the fluorescent microspheres (**A**). Zoom on 3 adjacent microspheres. The illumination of beads at 830 and 1,107 nm shows a spatial shift of the bead images (false colors) (**B**). After x, y, z adjustments, the bead images are merged (**C**). Please click here to view a larger version of this figure.

The final step to achieve the precise temporal adjustment to activate CARS can be easily realized by imaging olive oil drops (containing numerous C-H bonds[32]) and by moving slightly the mirrors of the delay line to complete the synchronization in time of both laser pulse trains. **Figure 4** shows images of an olive oil droplet delivered from the Ti:sapphire laser illumination only (**Figure 4A**) and from the OPO illumination only (**Figure 4B**). Both beams simultaneously applied induce a clear signal enhancement (**Figure 4C**) at 670 nm, which corresponds to a CARS signal from intrinsic carbon-hydrogen (C-H) stretching vibration with a Raman vibration range around 2,800 - 3,100 cm^{-1}. CARS signal (C) disappears when one the two beams is switched off. Since olive oil contains natural fluorophores[33], in particular chlorophyll molecules emitting in the range 650 - 670 nm, the weak signal in (A) and (B) is a multiphoton fluorescence process. The intensity of these signals is several orders of magnitude lower than the CARS signal. Therefore, it does not perturb the measurement of the CARS signal.

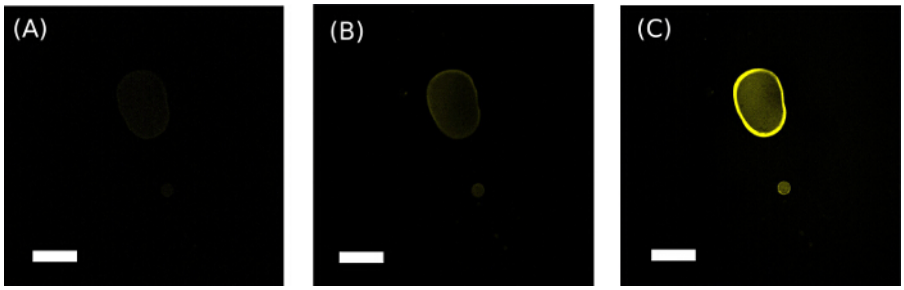

Figure 4. Final fine temporal adjustments for CARS signal outbreak. Olive oil droplets can be used to tune in time both beams by adjusting the delay line length with the linear translation stage with micrometer drive. Droplets under (**A**) 830 nm laser light only and under (**B**) 1,107 nm laser light only show a weak signal. Under simultaneous illumination (**C**), clear signal enhancement is observed, corresponding to the CARS signal. Scale bars are 100 µm. Raman vibration peak at 3,015 cm^{-1}. Please click here to view a larger version of this figure.

The myelin sheath is a biological structure produced by specific cells that wrap and condensate their plasma membrane around axons of neurons in central and peripheral nervous systems[34]. This sheath is highly enriched in different lipids. We used here the myelin sheaths of the sciatic nerve of a mouse. Transversal and longitudinal sciatic nerve cross-section segments have been stained for two-photon fluorescence imaging of myelin at 1,095 nm as shown in **Figure 5B** and **Figure 5E**, respectively. A fluoromyelin red dye, which has selectivity for myelin was used[35]. These samples have been simultaneously illuminated at 830 and at 1,095 nm and the CARS signal was observed (**Figure 5A** and **Figure 5D**). In **Figure 5A-C**, the circles correspond to myelin sheaths around axons (empty space inside the rings) in transversal cut. As shown in **Figure 5C** and **5F**, the same structure is found while overlapping CARS and fluorescence images. We conclude that similar level of details can be obtained with CARS and therefore without the use of fluorescent labeling.

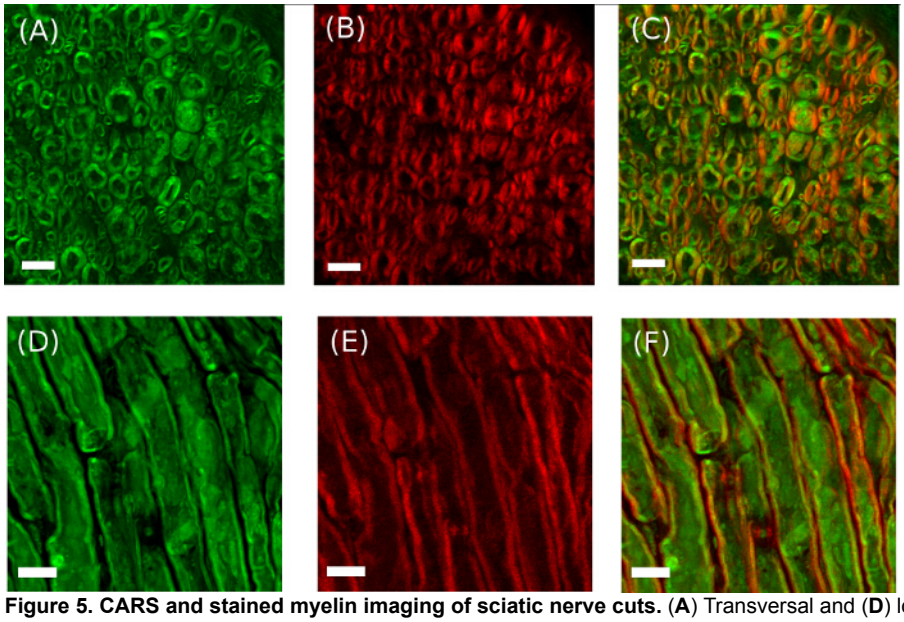

Figure 5. CARS and stained myelin imaging of sciatic nerve cuts. (**A**) Transversal and (**D**) longitudinal cuts of label-free CARS imaging of myelin sheaths. (**B**) Transversal and (**E**) longitudinal cuts of the same sample stained by the fluoromyelin red dye under two-photon fluorescence illumination at 1,095 nm. (**C**) Transversal and (**F**) longitudinal cut overlap of both images. Scale bars are 10 µm. Average optical powers were 5 mW at 830 nm and 16 mW at 1,095 nm for CARS signal. Average optical power was 8 mW at 1,095 nm for two-photon fluorescence imaging. Raman vibration peak at 2,915 cm^{-1}. CARS signal disappears by stopping the scan of one the laser or by moving the translation stage out of the Raman resonance. Please click here to view a larger version of this figure.

Additionally to CARS imaging, the available microscopy system allows to simultaneously generate second harmonic from the collagen fibers at the outer surface of the sciatic nerves. This additional image only requires the use of a different detector to record a signal at 550 nm (half the wavelength of the OPO) since a narrow band-pass filter at 670 nm is used for the CARS signal recording. **Figure 6** shows a contrast image of myelin sheaths depicted in false green color (CARS signal only in **Figure 6A**) surrounded by collagen fibers illustrated in false magenta color (SHG only in **Figure 6B**). CARS signal was achieved with average optical powers of 4 mW at 830 nm and 13 mW at 1,095 nm, while it required 50 mW at 1,095 nm to obtain the SHG signal. Therefore much lower optical energy is required to obtain CARS signal compared to SHG or THG (not shown) signals in our biological samples.

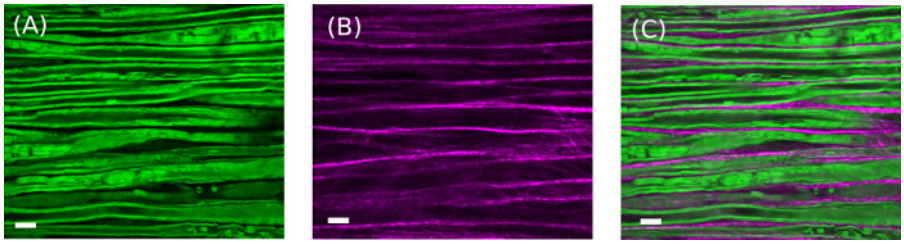

Figure 6. CARS and SHG imaging of mouse sciatic nerve. (**A**) CARS imaging, (**B**) SHG imaging and (**C**) simultaneous visualization of myelin by CARS imaging (in green false color) and of collagen by SHG imaging (in magenta) on the mouse sciatic nerve. Average optical powers were 4 mW at 830 nm and 13 mW at 1,095 nm for CARS. Average optical power was 50 mW at 1,095 nm for SHG. Scale bar is 10 µm. Raman vibration peak at 2,915 cm^{-1}. Please click here to view a larger version of this figure.

Discussion

The most challenging part of the work is the temporal synchronization of the laser beams. It requires a fast photodiode combined with a fast oscilloscope, but only a rough overlapping in time can be performed at first. Then a further adjustment of few cm is required. Finally, micrometer moves by a linear translation stage allows performing the final fine adjustment of the delay line length in order to trigger the CARS signal. This signal is maintained in a narrow range of around 20 micrometers, as observed by tuning the translation stage micrometer drive. It corresponds to a peak shift of the beams of around half of the pulse duration, *i.e.,* 140 fsec. The spatial overlapping of the two beams which is required for the CARS signal is similar to a normal beam alignment for such laser scanning microscope system.

The implementation of the delay line can be achieved in few weeks by biologists having a basic background in experimental optics or in collaboration with physicists. Special care has to be taken for the choice of the mirrors to minimize reflection losses. If the majority of the materials to build the delay line is affordable, the oscilloscope which is required is not a standard oscilloscope. Thus, since few days are enough to complete the temporal synchronization procedure, borrowing the oscilloscope from a physic laboratory appears to be the best option. Spatial overlapping can be time consuming since it demands the tuning of several mirrors and lenses (which can be motorized depending on the laser scanning system). Earlier CARS laser system based on two electronically synchronized Ti:sapphire laser had an issue with long term (tens of

minutes to hours) temporal pulse overlapping. This problem has been totally solved with OPO pumped with a unique laser source[20,21]. With such a laser system, and using firmly clamped optics, no temporal walk-off between pump and Stokes beams was observed over months of operation.

A major limitation of the CARS technique is that the CARS signal can occur without the presence of resonant molecules (from the solvent or the scatterers)[11]. This non-resonant background can limit the sensitivity. Ways to minimize this background include the configuration of detection (forward or backward detection), the laser characteristics (femtosecond or picosecond), the choice of the solution used to immerse the objective or image treatment. A backward detection allows to minimize the non-resonant background[11] as it was used in this work (**Figure 1**). Femtosecond Ti:sapphire lasers provide high peak intensities highly desirable for non-linear optical processes. However, in the spectral domain, the width of most Raman lines is smaller than the spectral width of a femtosecond pulse whereas it fits the spectral width of a picosecond pulse. Therefore the use of picosecond laser increases the ratio of resonant signal to non-resonant background. For C-H bonds in lipid, because of the high density of the bonds, the non-resonant background is negligible for a femtosecond laser. To reduce the background effect, the subtraction of a reference image recorded under off-resonant can also be applied (not done for this work).

Despite the utilization of near-infrared laser beams allowing deep penetration in tissue (200 - 300 microns), the practical penetration depth obtained in nerve imaging was around 50 microns with the experiments conducted in this work. However this parameter is heavily dependent of the biological tissue imaged and, because all myelinated fibers are aligned and concentrated in a small space, peripheral nerves probably do not constitute the best samples for evaluating this light penetration. In addition, few seconds are required to record high resolution images (1,024×1,024 pixels), which can limit the visualization of *in vivo* samples since even anesthetized, the breathing can induce slight movements.

CARS microscopy allows chemically specific selective imaging with a resolution close to the diffraction limit. This technique does not require any labeling, and since the Ti:sapphire laser is tunable from 700 to 1,000 nm and the OPO laser from 1,100 to 1,300 nm, it covers the entire spectrum region of molecular vibrations in biological systems (from 500 to 7,000 cm^{-1}). Thus, it is applicable and highly discriminative to DNA, proteins, lipids, or water, while the stronger signal arises from the lipid C-H stretching bond. Photodamage is also reduced due to the low level of laser power used to generate the CARS signal compared to the second-harmonic generation imaging. Since CARS imaging can be realized with low laser power and without invasive tags, it is therefore a tool of choice for *in vivo* studies.

Laser scanning microscopes with a femtosecond Ti:sapphire laser source combined with an OPO have become largely available for two-photon microscopy in many biological laboratories. Since the spatial synchronization is already implemented in these systems, the temporal overlapping procedure of the two beams described in this work brings an additional technique of microscopy without expensive additional equipment. Thus, the modified set-up allows for simultaneous imaging of cells or living tissue with Second or Third Harmonic Generation (SHG, THG), two-photon fluorescence and CARS. CARS technique has demonstrated great potential for *in vivo* imaging of live animals allowing the study of dynamical processes (without stains or genetic manipulations). Promising applications include *in vivo* label-free non-invasive lipid imaging, used for instance for real-time imaging of neuronal myelin in live spinal tissues[36], for studying lipid-related diseases (obesity, demyelinating and cardiovascular diseases)[37], human skin penetration mechanisms[22] or skin disorders[38]. We believe that future improvements will concern the use of special objective lenses, such as GRIN micro-objectives or miniature objective to enhance the penetration depth of the CARS signal.

Disclosures

The authors declare that they have no competing financial interests.

Acknowledgements

The authors want to thank Dr. Philippe Combette (IES, UM, Montpellier, France) for the loan of the fast oscilloscope and acknowledge financial supports from Montpellier RIO Imaging (MRI). HR acknowledges ANR grants France Bio Imaging (ANR-10-INSB-04-01) and France Life Imaging (ANR-11-INSB-0006) infrastructure networks for coherent Raman imaging developments. This work was mainly supported by an European Research Council grant (FP7-IDEAS-ERC 311610) and an INSERM - AVENIR grant to NT.

References

1. Valeur, B., & Berberan-Santos, M.N. *Molecular Fluorescence: Principles and Applications.* 2nd Edition. Wiley-VCH Verlag GmbH, (2012).
2. Denk, W., Strickler, J.H., & Webb, W.W. Two-photon laser scanning fluorescence microscopy. *Science.* **248** (4951), 73-76 (1990).
3. Moreaux, L., Sandre, O., & Mertz, J. Membrane imaging by second-harmonic generation microscopy. *JOSA B.* **17** (10), 1685-1694 (2000).
4. Zoumi, A., Yeh, A., & Tromberg, B.J. Imaging cells and extracellular matrix *in vivo* by using second-harmonic generation and two-photon excited fluorescence. *Proc. Natl. Acad. Sci. USA.* **99** (17), 11014-11019 (2002).
5. Yelin, D., & Silberberg, Y. Laser scanning third-harmonic-generation microscopy in biology. *Opt. Express.* **5** (8), 169-175 (1999).
6. Campagnola, P.J., Millard, A.C., Terasaki, M., Hoppe, P.E., Malone, C.J., & Mohler, W.A. Three-dimensional high-resolution Second-Harmonic Generation imaging of endogenous structural proteins in biological tissues. *Biophys. J.* **81** (1), 493-508 (2002).
7. Olivier, N., *et al.* Cell lineage reconstruction of early zebrafish embryos using label-free nonlinear microscopy. *Science.* **329** (5994), 967-971 (2010).
8. Farrar, M.J., Wise, F.W., Fetcho, J.R., & Schaffer C.B. *In vivo* imaging of myelin in the vertebrate central nervous system using third harmonic generation microscopy. *Biophys. J.* **100** (5), 1362-71 (2011).
9. Lim, H., Sharoukhov, D., Kassim, L., Zhang, Y., Salzer, J.L., & Melendez-Vasquez, C.V. Label-free imaging of Schwann cell myelination by third harmonic generation microscopy. *Proc. Natl. Acad. Sci. U.S.A.* **111** (50), 18025-18030 (2014).
10. Strupler, M., Pena, A.M., Hernest, M., Tharaux, P.L., Martin, J.L., Beaurepaire, E., & Schanne-Klein, M.C. Second harmonic imaging and scoring of collagen in fibrotic tissues. *Opt. Express.* **15** (7), 4054-65 (2007).
11. Cheng, J.X., & Xie X.S. Coherent anti-Stokes Raman scattering microscopy: Instrumentation, theory, and applications. *J. Phys. Chem. B.* **108** (3), 827-840 (2004).

12. Volkmer, A. Vibrational imaging and microspectroscopies based on coherent anti-Stokes scattering microscopy. *J. Phys. D: Appl. Phys.* **38**, R59-R81 (2005).
13. Evans, C.L., & Xie X.S. Coherent anti-Stokes Raman scattering microscopy: chemical imaging for biology and medicine. *Annu. Rev. Anal. Chem.* **1**, 883-909 (2008).
14. Mukamel, S. *Principles of nonlinear optical spectroscopy.* Oxford University Press, New York, (1995).
15. Duncan, M.D., Reintjes, J., & Manuccia, T.J. Scanning coherent anti-Stokes Raman microscope. *Opt. Lett.* **7** (8), 350-352 (1982).
16. Zumbusch, A., Holtom, G.R., & Xie X.S. Three-dimensional vibrational imaging by coherent anti-Stokes Raman scattering. *Phys. Rev. Lett.* **82** (20), 4142-4145 (1999).
17. Folick, A., Min, W., & Wang, M.C. Label-free imaging of lipid dynamics using Coherent Anti-Stokes Raman Scattering (CARS) and Stimulated Raman Scattering (SRS) microscopy.*Curr. Opin. Genet. Dev.* **21** (5), 585-590 (2011).
18. Wang, P., Liu, B., Zhang, D., Belew, M.Y., Tissenbaum, H.A., & Cheng J.X. Imaging lipid metabolism in live Caenorhabditis elegans using fingerprint vibrations. *Angew. Chem. Int. Ed. Engl.* **53** (44), 11787-11792 (2014).
19. Min, W., Freudiger, C.W., Lu, S., & Xie X.S. Coherent nonlinear optical imaging: beyond fluorescence microscopy. *Annu. Rev. Phys. Chem.* **62**, 507-530 (2011).
20. Cheng, J.X., Jia, Y.K., Zheng, G., & Xie X.S. Laser-scanning coherent anti-Stokes Raman scattering microscopy and applications to cell biology. *Biophys J.* **83** (1), 502-509 (2002).
21. Chiu, W. S., Belsey, N. A. N., Garrett, L., Moger, J., Delgado-Charro, M. B., & Guy, R. H. Molecular diffusion in the human nail measured by stimulated Raman scattering microscopy. *Proc Natl. Acad. Sci. U.S.A.* **112**, 7725-7730 (2015).
22. Chen, X., Grégoire, S., Formanek, F., Galey, J.-B., & Rigneault, H. Quantitative 3D molecular cutaneous absorption in human skin using label free nonlinear microscopy. *J. of Control. Release.* **200**, 78-86 (2015).
23. Kano, H., & Hamaguchi, H. *In vivo* multi-nonlinear optical imaging of a living cell using a supercontinuum light source generated from a photonic crystal fiber. *Opt. Express.* **14** (7), 2798-2804 (2006).
24. Brustlein, S., Ferrand, P., Walther, N., Brasselet, S., Billaudeau, C., Marguet, D., & Rigneault, H. Optical parametric oscillator-based light source for coherent Raman scattering microscopy: practical overview. *J. Biomed. Opt.* **16**(2), 021106 (2011).
25. Chen, H. *et al.* A multimodal platform for nonlinear optical microscopy and microspectroscopy. *Opt. Express.* **17** (3), 1282-1290 (2009).
26. Yue, S., Slipchenko, M.N., & Cheng, J.X. Multimodal nonlinear optical microscopy. *Laser Photonics Rev.* **5** (4), 496-512 (2011).
27. Sun, Q., Li, Y., He, S., Situ, C., Wu, Z., & Qu, J.Y. Label-free multimodal nonlinear optical microscopy reveals fundamental insights of skeletal muscle development. *Biomed Opt Express.* **5** (1), 158-166 (2013).
28. Le, T.T, Langohr, I.M., Locker, M.J., Sturek, M., & Cheng, J.X. Label-free molecular imaging of atherosclerotic lesions using multimodal nonlinear optical microscopy. *J. Biomed. Opt.* **12** (5), 054007 (2007).
29. Ellis, D.I., Cowcher, D.P., Ashton, L., O'Hagana, S., & Goodacre, R. Illuminating disease and enlightening biomedicine: Raman spectroscopy as a diagnostic tool. *Analyst.* **138**, 3871-3884 (2013).
30. *A•P•E Angewandte Physik & Elektronik GmbH.* Germany, http://www.ape-berlin.de/en/page/calculator (2015).
31. Ozçelik, M. *et al.* Pals1 is a major regulator of the epithelial-like polarization and the extension of the myelin sheath in peripheral nerves. *J Neurosci.* **30**(11), 4120-4131 (2010).
32. Heinrich, C., Hofer, A., Ritsch, A., Ciardi, C., Bernet, S., & Ritsch-Marte, M. Selective imaging of saturated and unsaturated lipids by wide-field CARS-microscopy. *Opt. Express.* **16** (4), 2699-708 (2008).
33. Kyriakidis, N.B., & Skarkalis, P. Fluorescence spectra measurement of olive oil and other vegetable oils. *J. AOAC Int.* **83** (6), 1435-1439 (2000).
34. King, R. Microscopic anatomy: normal structure. *Handb. Clin. Neurol.* ***115***, 7-27 (2013).
35. Monsma, P.C., & Brown, A. FluoroMyelin Red is a bright, photostable and non-toxic fluorescent stain for live imaging of myelin. *J. Neurosci. Methods.* **209** (2), 344-350 (2012).
36. Wang, H., Fu, Y., Zickmund, P., Shi, R., & Cheng, J.X. Coherent anti-stokes Raman scattering imaging of axonal myelin in live spinal tissues. *Biophys. J.* **89** (1), 581-591 (2005).
37. Wang, H.W., Fu, Y., Huff, T.B., Le, T.T., Wang, H., & Cheng J.X. Chasing lipids in health and diseases by coherent anti-Stokes Raman scattering microscopy. *Vib. Spectrosc.* **50** (1), 160-167 (2009).
38. Jung, Y., Tam, J., Jalian, H.R., Anderson, R.R., & Evans, C.L. Longitudinal, 3D *in vivo* imaging of sebaceous glands by coherent anti-stokes Raman scattering microscopy: normal function and response to cryotherapy. *J. Invest. Dermatol.* **135** (1), 39-44 (2015).

